TOPICS IN HIGH ENERGY PERTURBATIVE QCD INCLUDING INTERACTIONS WITH NUCLEAR MATTER

A. H. Mueller
Department of Physics, Columbia University
New York, N.Y. 10027

Abstract

In these lectures some current topics in QCD are discussed. These topics include: (i) Form factors and elastic scattering. (ii) Nuclear A-dependence of QCD cross sections. (iii) Heavy particle production at high energy. (iv) Soft hadron production in QCD jets. (v) Soft gluons and factorization in μ-pair production.

This research was supported in part by the U.S. Department of Energy.

I. Form Factors and Elastic Scattering

The study of elastic form factors and wide angle elastic scattering in perturbative QCD has led to a very satisfying picture of these processes.[1] At present it is felt that a relatively complete description of the large momentum transfer dependence has been obtained. Perhaps even more importantly, a very simple physical picture has emerged. On the negative side, however, it appears very hard to get truly quantitative tests of QCD from exclusive processes.

Let me begin by first giving the physical picture which now appears to describe large momentum transfer exclusive processes. Then I would like to briefly discuss a possible experiment which could be used to test this physical picture, and which at the same time gives information on some nuclear properties not easily obtained by other means.

A. Meson Form Factors[2-7]

As an example of a form factor at large momentum transfer consider the process shown in Fig. 1 where a π of momentum p is hit by a hard virtual photon and turns into a pion of momentum p'. We suppose that $Q^2 = (\vec{p} - \vec{p}')^2 = 2\vec{p}^{\,2}(1 - \cos\theta)$ with θ fixed as Q^2 becomes large. A straightforward interpretation of QCD calculations leads to the following picture of the process.

(i) The quark-antiquark pair making up the π begin to contract to a small transverse size at a time $t = T_i \sim p/\mu^2$ before the hard photon hits the π. If the π has virtual gluons or sea quark-antiquark pairs present, these begin to be absorbed around the time $t \approx T_i$. This contraction continues until the quark-antiquark pair is within a size $|\Delta\vec{x}| \lesssim 1/Q$ just before the hard photon hits.

(ii) At $t = 0$ the hard photon hits either the quark or the antiquark in the π. After the quark, say, is hit it begins to separate from the antiquark. Within a time $t \approx 1/Q$ there occurs a hard interaction between the quark and the antiquark in order that they not separate giving an inelastic reaction. After the hard interaction the quark and antiquark are moving parallel to each other.

(iii) After $t = O(1/Q)$ until $t = T_f \sim p/\mu^2$ the quark-antiquark system expands to a normal transverse size. When the quark-antiquark pair has attained a transverse size of order $1/\mu$, with $\mu \approx 350$ MeV, gluons and additional quark-antiquark pairs appear. This system corresponds to the normal wave function of the π.

In terms of a formula

$$F_\pi(Q^2) \xrightarrow[Q^2\to\infty]{} 16\pi f_\pi^2 \frac{\alpha(Q^2)}{Q^2}\left[1 + \sum_{N=2,4,6}^{\infty} C_N \left(\ln\frac{Q^2}{\mu^2}\right)^{-\gamma_N}\right]^2 . \qquad (1)$$

The $\frac{\alpha(Q^2)}{Q^2}$ factor comes from stage (ii), the hard scattering. A factor of

$f_\pi\left[1 + \sum C_N (\ln \frac{Q^2}{\mu^2})^{-\gamma_N}\right]$ comes from the collapse of the π wave function in stage (i) and an identical factor comes from stage (iii). The γ_N are positive and calculable. The C_N reflect details of how the pion wave function matches onto the QCD evolving quark-antiquark system and are only calculable after detailed assumptions about non-perturbative QCD are made.

B. Wide Angle Elastic Scattering

As an example of wide angle elastic scattering I shall discuss π-π scattering. Let me begin by discussing the contrasting power counting rules suggested by Brodsky and Farrar[8] and by Landshoff.[9]

In the Brodsky-Farrar picture, elastic scattering proceeds much as in the picture we have just outlined for the pion form factor. Refer to the graph shown in Fig. 2. According to Brodsky and Farrar, before the scattering the valence quark-antiquark pair (3, 4) in the pion comes within a transverse distance $|\Delta \underline{x}| \lesssim 1/\sqrt{s}$ as does the pair (1, 2). The Fock states of the two pions, in the center of mass system, are supposed to consist only of their quark-antiquark valence pairs just before the hard collision. Upon colliding, two interactions between the pions are necessary in order to turn both the quark and the antiquark through an angle θ. A simple counting of variables then indicates the necessity of a further hard interaction in order that the outgoing quark-antiquark systems have low masses. Dimensional counting for these various hard scatterings, three of them, gives $\frac{d\sigma}{dt} \underset{\theta \text{ fixed}}{\underset{s\to\infty}{\longrightarrow}} \frac{1}{s^6} f(\theta)$.

In the Landshoff picture, see Fig. 3, the pions also consist of only their quark-antiquark valence pairs. However, now one views the quark and the antiquark in a particular pion as not being close together in transverse coordinate space. (In momentum space this means that the quark and antiquark are not very far off mass shell.) There are supposed to occur two scatterings of almost identical angles which turn the pairs through an angle θ, leaving them in low mass systems. That is $\theta(1,1') \approx \theta(2,2') \approx \theta(3,3') \approx \theta(4,4')$. A power counting for such scatterings leads to $\frac{d\sigma}{dt} \underset{\theta \text{ fixed}}{\underset{s\to\infty}{\longrightarrow}} \frac{1}{s^5} \tilde{f}(\theta)$.

Thus the Landshoff type of scattering would seem to dominate wide angle elastic scattering. However, there is yet another effect in the Landshoff picture. The valence pairs in the pions are not so close together and hence do not form a locally neutral system in color. Thus it is unlikely that collinear and soft gluons will be absent before the hard scatterings. However, gluons must be absent if the scattering is to be purely elastic. In general the price one pays for picking out a particular piece of the wave function having no collinear or soft gluons is a Sudakov factor. (In the Brodsky-Farrar type of scattering the pairs in each pion are close together and so form a local color singlet. A color singlet does not need to have a gluon

cloud and so one expects no Sudakov suppression in that case.

In fact there are Sudakov corrections to the Landshoff graphs. They have the effect of forcing the valence pairs to be close together, though not quite so close as in the original Brodsky-Farrar picture. It turns out[1] that $\frac{d\sigma}{dt} \to \frac{1}{s^5} s^{-4c \ln \frac{4c+1}{4c}}$, as far as power dependences are concerned, with $c = \frac{4c_F}{11 - \frac{2}{3}n_f}$. The final physical picture is very close to the view of Brodsky and Farrar.

C. Almost Elastic Nuclear Reactions: $\pi + A \to \pi' + P' + (A-1)$

I would now like to discuss an example of wide angle elastic scattering in a peculiar context. The reaction involves the scattering of, say, a π of momentum $\vec{k}$ on a nucleus, A. The final state is supposed to be a π of momentum $\vec{k}'$, a proton of momentum $\vec{p}'$ and a nucleus, A - 1. It is not necessary that the nucleus, A - 1, be in its ground state, but it is required that there be no nuclear breakup and that no soft pions be produced. In effect, then, we are looking at an elastic reaction $\pi(\vec{k}) + \text{Nucleon}\,(\vec{p}) \to \pi(\vec{k}') + P(\vec{p}')$ with the nucleus playing no role at all except as a source of Nucleon $(\vec{p})$. Such a reaction would seem difficult to realize. One might expect the incoming pion, or even the outgoing pion and proton, to strongly interact with the nucleus producing many pions along with a complete breakup of the nucleus.

A moment's thought, however, convinces one that it is not necessary to have nuclear breakup, at least if the view of wide angle elastic scattering presented earlier in this section is correct. The nuclear scattering is viewed to proceed, in the rest system of the nucleus, in the following manner. Before the $\pi(\vec{k})$ reaches the nucleus it is supposed to become a quark-antiquark pair of small transverse size. We know that the probability of that happening is not small. The quark-antiquark system should be able to freely pass through nuclear matter because it is color neutral in a fairly local way. Thus the $\pi(\vec{k})$ moves into the nucleus and at some point a hard scattering occurs. (The hard scattering penetrates to such short transverse distances that the π no longer looks color neutral.) Immediately after the elastic scattering a quark-antiquark system of momentum $\vec{k}'$ heads out of the nucleus. This pair is of small transverse size after the hard scattering and is only supposed to obtain the normal size of a pion, which it becomes, after it has left the nucleus. A three quark system, also small in size, leaves the hard scattering and expands to the size of a normal proton outside the nucleus giving the final proton of momentum $\vec{p}'$. For example, if the incoming pion is a π^+ and the final pion is a π^+ we might expect

$$\frac{d\sigma}{dt} = Z \frac{d\sigma_{\pi^+ p \to \pi^+ p}}{dt} \qquad (2)$$

though we shall see a little later that Eq. (2) must be modified to take into account Fermi-motion effects.

What are the essential ingredients for such a reaction to work? (i) The initial momentum, k, of the pion must be large enough that the collapse of the π to a small quark-antiquark system takes place outside the nucleus. In the rest system of the π such a collapse takes a time $\tau \approx 1/\mu$ with $\mu \approx 350$ MeV. The time dilatation factor leads to the requirement $\frac{k}{m_\pi \mu} >> 2R$ or $k >> 3$ GeV for a large nucleus. (ii) The final pion momentum must also obey $k' >> 3$ GeV. (iii) The requirement that the three quark system stay small until it gets outside the nucleus gives the most stringent condition, $\frac{p'}{m_p \mu} >> 2R$ or $p' >> 25$ GeV. (iv) The momentum transfer must be much larger than the inverse of a normal hadronic size. Momentum transfers of more than 3-4 GeV should certainly be sufficient while momentum transfers of 1 GeV or so may already be large enough. What is required here is simply that the various neutral quark systems be small enough so that nuclear matter is transparent. We need not require that the hard scattering be described by any particular QCD formula. The above constraints can be met at a pion laboratory momentum of perhaps 50 GeV or so for a large nucleus. For smaller nuclei the necessary incident momentum can be much less.

There is perhaps another reason for considering such reactions, in addition to the insight they may add concerning QCD. Let us suppose that $\vec{k}$ is along the z-axis. If k, p' and the angles at which $\vec{k}'$ and $\vec{p}'$ come from the collision center can be measured to within a few percent, one can reconstruct the momentum $\vec{p}$ of the struck nucleon in the nucleus. Then the formula which should result is

$$\frac{d\sigma(\vec{p}', \vec{k}'; \vec{k})}{dt} = \left[Z \frac{d\sigma_{\pi p \to \pi' p'}(s,t)}{dt} + (A - Z) \frac{d\sigma_{\pi N \to \pi' p'}(s,t)}{dt} \right] f(p) \quad (3)$$

where $s = (p'_\mu + k'_\mu)^2$, $t = (k'_\mu - k_\mu)^2$, $|\vec{p}| = p$ and $f(p)$ is the probability that a nucleon of momentum p be found in the nucleus. We have used the normalization $\int d^3\vec{p}\, f(p) = 1$. Depending on the initial and final pion charges, one or the other of the two terms on the right hand side of Eq. (3) may be zero.

For small p, $f(p)$ is believed to be fairly well understood. If it turns out that Eq. (3) works well for small p, then it is natural to use this equation to determine $f(p)$ for larger values of p, say a GeV or so. So far as I know, $f(p)$ has not been well determined for large values of p. Thus one can use the above reaction to measure the distribution of nucleon momenta in the nucleus.

II. Nuclear A-Dependence of Cross Sections and Jet Evolution in Nuclear Matter

A. A-Dependence of Structure Functions

It has been known for many years that the cross section for high energy photons to interact with nuclei does not vary as A times the photon nucleon cross section. At high energies $A_{eff}/A \approx 0.6\text{-}0.7$ for a lead target. However, until recently there was no evidence for shadowing of virtual photons in the deeply inelastic region. Such evidence has now been found[10] which indicates that virtual photons exhibit as much shadowing as real photons in the Fermilab energy regime so long as $Q^2 \lesssim 2\text{-}3\ \text{GeV}^2$. The range of strong shadowing, $A_{eff}/A \approx 0.6$, corresponds to $x \lesssim 0.01$. Whether this shadowing is only a function of x or whether there is a Q^2-dependence is not known at present, but could be determined at Fermilab in the next few years.

There are two distinct, but presumably equivalent, ways to view shadowing effects in deeply inelastic scattering off nuclei. Let us begin by taking the nucleus at rest. If P is the nuclear momentum, then $P = (M, 0, 0, 0)$ and p, the momentum per nucleon, is given by $p = (M/A, 0, 0, 0) \approx (m, 0, 0, 0)$ with m the nucleon rest mass. For large Q^2 and small x the photon momentum takes the form $q \approx (q - mx, 0, 0, q)$ where x is defined with respect to the nucleon momentum. When x is small the virtual photon has a relatively long time scale for interaction in this frame.[11-14] We may estimate this time scale, τ, by equating τ to the inverse of the energy difference between the virtual photon energy and the energy of a real photon having the same three-momentum. This is a standard uncertainty principle argument. One finds

$$\tau \approx \frac{1}{q - (q - mx)} = \frac{1}{mx} \quad .$$

The virtual photon can either be in a state of one bare photon or in a virtual hadronic state. The typical time for changing from one such state to another is τ. If the virtual photon is in the state consisting of a bare photon when it reaches the front of the nucleus, there will be no interaction at all if $\frac{1}{mx} > 2R$. If the photon is in a virtual hadron state, S, then the cross section for the process will be proportional to the cross section for the state S to interact with the nucleus. Thus one may write,[11-14] see Fig. 4,

$$\sigma_{\gamma A}^{in} = \sum_S |(S \mid \gamma)|^2 \sigma_{SA}^{in}$$

where $\sigma_{\gamma A}^{in}$ is the inelastic virtual photn-nucleus cross section, S is any hadronic state directly communicating with the photon, and $|(S \mid \gamma)|^2$ represents the probability that the virtual photon is in the hadronic state S. σ_{SA}^{in} is the inelastic cross section for the virtual hadronic state S to interact with the nucleus, A. (The calculation of $|(S \mid \gamma)|^2$ is non-

trivial and will not be discussed in detail in these lectures.)

Whether σ_{SA} is proportional to A or whether there is strong shadowing depends on the transverse size of the state S. If S is small, then that state will interact weakly with nucleons and there will be little shadowing. If S has a transverse size comparable to that of a physical hadron, there should be considerable shadowing. We shall return soon to a more detailed discussion as to how much shadowing is to be expected.

Let us now look at deeply inelastic scattering off nuclei in a frame where the nucleus is going very fast. We take $p \approx (p + m^2/2p, 0, 0, p)$ and $q = (q_0, \underline{q}, 0)$ with p large and $\underline{q}^2 = Q^2$. In addition q_0 is determined to be $q_0 = Q^2/2px \ll |\underline{q}|$. In this standard infinite momentum frame, illustrated in Fig. 5, the virtual photon simply measures the quark distribution functions of the nucleus. $\nu W_2^A(x, Q^2) = \sum_\alpha \ell_\alpha^2 \times P_A^\alpha(x, Q^2)$ where ℓ_α is the charge of the α-quark or antiquark and $P_A^\alpha(x, Q^2)$ is the number density of α-quarks in the nucleus. If there is no shadowing

$$P_A^\alpha(x, Q^2) = Z P_{proton}^\alpha(x, Q^2) + (A - Z) P_{neutron}^\alpha(x, Q^2) .$$

For small x, the only region for which shadowing is possible, shadowing means that there is a depletion in the number density of sea quarks and antiquarks from the number density one would get by adding the contributions from all the nucleons independently. Thus shadowing measurements are direct measurements of the sea quark components of the nuclear wave function.

(1) The Naive Parton Model

In the naive parton model one can definitively answer the question as to how much shadowing should be present in deeply inelastic scattering experiments. Let me give the argument in terms of both of the frames which have been considered so far. In the nuclear infinite momentum frame the valence quarks occupy a longitudinal size $\Delta z_v \approx 2R \frac{m}{p}$ as illustrated in Fig. 6. The longitudinal size of a gluon or sea quark of momentum k is $\Delta z \approx 1/k_z$. When $1/k_z > 2R \frac{m}{p}$ or $x < \frac{1}{2Rm}$ all sea quarks having such x values, at a fixed impact parameter, overlap spatially. (For lead $x \lesssim \frac{1}{2Rm}$ means $x \lesssim 0.01$.) Such sea quarks are really a property of the nucleus rather than of the individual nucleons. If one were to assume that the number density of such sea quarks is obtained simply by adding the number densities of the individual nucleons a number density proportional to $A^{1/3}$, for a fixed impact parameter, would be obtained, the case of no shadowing. But, physically this is very unreasonable! How can one make the number density become larger and larger, by increasing A, without having the quarks and antiquarks disappear through annihilation? (If the sea quarks and antiquarks had a very small transverse spread they would interact only weakly, and very large number densities would be possible. However, in the naive parton model the transverse spread of a given

quark is about 1/350 MeV, not a small number.) One would naturally expect a limit to the number density of sea quarks in the regime $x \sim 1/2mR$ as A increases, and this limit should be determined only by the quark and gluon properties independently of the parent nucleons.

In the rest frame of the nucleus we may view deeply inelastic scattering in the naive parton model as shown in Fig. 7. Let us write the state S', which the virtual photon first goes into, as a quark of momentum $\vec{k}$ and an antiquark of momentum $\vec{q} - \vec{k}$. The energy of that state is

$$E_{S'} = \sqrt{(\vec{q} - \vec{k})^2 + m^2} + \sqrt{\vec{k}^2 + m^2} \approx q + \frac{\underline{k}^2 + m^2}{2(q-k)} + \frac{\underline{k}^2 + m^2}{2k} .$$

The energy of the virtual photon is $E_q = q - mx$. The energy denominator which occurs in evaluating the transition probability for the photon to go into the quark antiquark state is

$$\frac{1}{(E_S - E_q)^2} = \frac{1}{\left(\frac{\underline{k}^2 + m^2}{2k} + \frac{\underline{k}^2 + m^2}{2(q-k)} + mx\right)^2} .$$

Now in the parton model $\underline{k}^2$ is limited, say by m^2. If $k \ll m/x$ the state S' is suppressed due to the growth of the energy denominator. If $k \gg m/x$ the contribution is suppressed due to the small scattering cross section of k on the target. Thus, $k \approx m/x$.

We may view the deeply inelastic cross section as a probability, of order one, for the creation of a quark-antiquark state times the cross section for the quark to scatter on the nucleus.[15] (The antiquark, which we have chosen to be the fastest of the quark-antiquark pair, cannot interact with the nucleus (in a light cone axial gauge) due to the slowing of the antiquark's rate of interaction caused by its large momentum. This time dilation factor is the source of interactions with the $q - k$ line, higher twist contributions, being down by a power of Q^2.) The transverse momentum of the quark, $\underline{k}$, is limited in the parton model which means that the transverse spread of the quark is of order $1/m$. If $x \lesssim 1/2Rm$ the state S' is formed before the virtual photon reaches the nucleus and a cross section proportional to πR^2 is expected as the quark should act much like a hadron.

In the naive porton model it is clear that one expects strong shadowing when $x \lesssim 1/2Rm$. Shadowing should begin when $x \lesssim 1/dm$ with d a typical intranuclear spacing. Thus for heavy nuclei one expects considerable shadowing when $x \lesssim 0.01$. This view is strongly supported by the experiment of Goodman *et al.*

(2) Deeply Inelastic Scattering in QCD

Our discussion of nuclear deeply inelastic scattering in terms of the parton model relied heavily on having a limited transverse momentum for quarks and gluons. For example, in the

fast nuclear frame, there would be no difficulty in having sea quarks and antiquarks overlap in the longitudinal direction if their spread in transverse space is small enough (large enough transverse momentum) so that they overlap little in three-dimensional space. A thorough theoretical discussion of shadowing in QCD is too complex to be presented here; however a qualitative discussion may give some insight into the issues which are involved. We should emphasize, though, that the naive parton model should give a reasonable guide as to what to expect experimentally. The QCD discussion should be a refinement, but not a negation, of the predictions of the parton model.

We begin by considering the Altarelli-Parisi equation

$$\frac{\partial}{\partial \ln Q^2} P_A(x, Q^2) = -\int_x^1 \frac{dx'}{x'} P_A(x', Q^2)\, \gamma\left(\frac{x}{x'}, g^2(Q^2)\right) \qquad (4)$$

for the nuclear parton number densities. In general γ is a matrix whose rows and columns represent gluons and the various flavors of quarks and antiquarks. A solution to Eq. (4) is given by

$$P_A(x, Q^2) = \int_x^1 \frac{dx'}{x'} P_A(x', Q_0^2)\, K\left(\frac{x}{x'}, Q^2, Q_0^2\right) \qquad (5)$$

where K may be represented as

$$K\left(\frac{x}{x'}, Q^2, Q_0^2\right) = \left(x' \left| \mathcal{P}\, e^{-\int_{Q_0^2}^{Q^2} \frac{d\lambda^2}{\lambda^2} \gamma(g^2(\lambda^2))} \right| x\right) . \qquad (6)$$

In Eq. (6) $\mathcal{P}$ stands for a λ^2 path ordering of the operator γ. In addition to being a matrix in quark flavor and gluon space, γ is an operator in x space such that

$$\left(x' \mid \gamma(g^2(\lambda^2)) \mid x\right) = \Theta\left(\frac{x'}{x} - 1\right) \gamma\left(\frac{x}{x'}, g^2(\lambda^2)\right) . \qquad (7)$$

It is possible to gain an intuitive picture of Eq. (6) if we view γ as an imaginary time Hamiltonian. K can be written as a sum over all paths, $x(Q^2)$, much as is often done for a one-dimensional quantum mechanical problem. In Fig. 7 some typical paths are shown. The paths shown there in $\ln 1/x'$ versus $\ln \lambda^2$ are monatonic because of the step function in Eq. (7). If these paths are read from left to right they correspond to the evolution of quarks and gluons from some non-perturbative distribution, $P_A(x, Q_0^2)$, in the nucleus to a final parton distribution $P_A(x, Q^2)$ which is measured by the virtual photon in a deeply inelastic scattering. (This is a description in the fast nuclear reference frame.) For example, following path ① from left to right in Fig. 7, a valence quark in the nucleus evolves to large Q^2 while remaining at large values of x. Then, after having reached large values of Q^2, it evolves to small values of x at which point it is struck by the hard virtual photon. In following such an

evolution the quarks and gluons first become small in transverse size before they overlap in longitudinal space. No shadowing is expected from an evolution following a path like ①. Path ②, on the other hand, corresponds to beginning with a gluon or sea quark at Q_0^2 and at very small x. This quanta then evolves to large Q^2 and is struck by the virtual photon. If $Q_0^2 \lesssim 1\ \mathrm{GeV}^2$ we expect considerable spatial overlap before the evolution to small size occurs. Path ② should correspond to strong shadowing. We can also interpret path ② by reading Fig. 7 from right to left. In this case we take the frame where the nucleus is at rest. In this frame the photon first turns into a quark-antiquark pair. Path ② follows the evolution of the quark which finally strikes the nucleus. This quark has a mass Q_0 and momentum proportional to Q_0/x' when it is considered to scatter off the nucleus. (x' is the point where path ② intersects the line $\ln\lambda^2 = \ln Q_0^2$ in Fig. 7.) Since a nearly on-shell quark having large momentum should have strong shadowing, we again expect path ② to exhibit considerable shadowing. The process as viewed in the rest frame of the nucleus, and evolving along path ②, is shown in Fig. 8.

Let us write Eq. (5) as

$$P_A(x, Q^2) = \int_{\frac{1}{2Rm}}^{1} P_A(x', Q_0^2)\, K\left(\frac{x}{x'}, Q^2, Q_0^2\right) + \int_{x}^{\frac{1}{2Rm}} \frac{dx'}{x'} P_A(x', Q_0^2)\, K\left(\frac{x}{x'}, Q^2, Q_0^2\right) = P_A^{①} + P_A^{②}. \tag{B}$$

The term whose integral runs between $1/2Rm$ and 1, $P_A^{①}$, should show little shadowing, while $P_A^{②}$ should show considerable shadowing. In QCD shadowing is not simply a function of x versus R as it is in the parton model. Nevertheless, it is clear that we should expect shadowing even for large values of Q^2 when x is small. A detailed quantitative discussion of shadowing on nuclei requires a knowledge of $\gamma(x, g^2)$ when x is small and a knowledge of $P_A(x, Q_0^2)$ when $Q_0^2 \approx 2\ \mathrm{GeV}^2$, say.

B. A- Dependence of μ- Pair Production[16]

Consider massive μ- pair production in a hadron-nucleus collision as illustrated in Fig. 9. In the QCD improved parton model we expect

$$\frac{d\sigma}{dQ^2} = \int \frac{d\sigma}{d^4q}\, d^2q_t = \frac{8\pi\alpha^2}{3n_c(Q^2)^2} \sum_{\alpha} e_\alpha^2 \left[x_1 P^{\alpha}(x_1, Q^2)\, x_2 P_A^{\bar{\alpha}}(x_2, Q^2) + x_1 P^{\bar{\alpha}}(x_1, Q^2)\, x_2 P_A^{\alpha}(x_2, Q^2)\right]. \tag{9}$$

$P^{\alpha}(x, Q^2)$ is the number density for quarks of type α in the hadron while $P_A^{\alpha}(x, Q^2)$ is the number density for quarks in the nucleus. x_1 and x_2 are the usual momentum fractions carried

by the quark and antiquark which annihilate to give the μ-pair. The question we wish to discuss here is at what values of x_i and Q^2 should we expect Eq. (9) to hold and at what values of the parameters should we expect shadowing to occur.

It is clear that we cannot expect Eq. (9) to be correct when R is very large and p_1 and p_2 are fixed. In such a circumstance the hadron sees only the front end of the nucleus with which it collides. View the reaction in the rest system of the nucleus. In this frame we would like the process to take place by the line k_1 reaching into the center of the nucleus and striking a line k_2 to produce the μ-pair. Or, in case x_2 is small, the link k_1 first emits the μ-pair and then turns into the line $-k_2$ which subsequently interacts with the nucleus. However, we know such a simple description cannot be completely correct. Even when k_1 is large it may interact via soft gluon exchange with the nucleus if k_1^2 is not large. It will be argued in Sec. V that such interactions likely violate factorization,[16] even for hadron + hadron $\to \mu^+ + \mu^- + X$, in perturbation theory though these non-factorizing effects should be suppressed by Sudakov factors at large Q^2. Besides interacting by means of soft gluon exchanges, the line k_1 has the possibility of turning into a hadronic system which can be absorbed by the nucleus. The line k_1 can completely change its character on a time scale

$$\tau \approx \frac{|\vec{k}_1|}{\kappa_1^2} \quad , \qquad \kappa_1^2 = |k_1^2| \quad . \tag{10}$$

However, in order that k_1 change into an hadronic system which can be absorbed by the nucleus, it is necessary that $\kappa_1^2 \approx \mu^2 = (350\ \text{MeV})^2$ since normal hadronic interactions do not involve hard scatterings which would be required to make $\kappa_1^2/\mu^2 \gg 1$. Thus $\tau \approx k_1/\mu^2 = x_1 p_1/\mu^2$. Now $Q^2 = 2x_1 x_2 p_1 m$ so that the requirement that the k_1 line not turn into an hadronic system which can interact strongly with the nucleus is $\tau \gtrsim 2R$ or

$$\frac{Q^2}{\mu^2} \gtrsim 4Rm\, x_2 \quad . \tag{11}$$

For $x_2 = \frac{1}{2}$ and for lead this requires $Q^2 \gtrsim 10\ \text{GeV}^2$.

Our result, Eq. (11), is somewhat different than the conclusion of Ref. 16 where $Q^2 \gtrsim \text{const}\ A^{2/3}$ is required before radiation induced by the passage of the k_1 line through the nucleus is small. The source of this difference is easy to see. Bodwin, Brodsky and Lepage (BBL) argue that the k_1 line, as it passes through the nucleus, picks up a transverse momentum and a mass $\underline{k}_1^2 \alpha \kappa_1^2$ from random soft multiple scatterings and that this causes κ_1^2 to become as large as $A^{1/3}$. Such an effect would immediately give an additional $A^{1/3}$ on the right hand side of our Eq. (11). However, as shall be discussed in more detail a little later on, an off-shell line interacts only weakly with nuclear matter, the strength of the interaction

decreasing as a power of the off-shellness. Thus we feel that a quark, or gluon, line cannot be pushed far off shell by a series of soft scatterings since the soft scatterings become very weak as the quark, or gluon, line goes more than a little off-shell.

Given (11) for the validity of Eq. (9), the amount of shadowing present then follows directly from our discussion of deeply inelastic scattering since the $P_A^\alpha(x, Q^2)$ is exactly the one discussed there. Strong shadowing should occur when x_2 is small, say $x_2 \lesssim 0.01$.

C. Jet Evolution in Nuclear Matter

In this section we shall briefly discuss the evolution of QCD jets in nuclear matter. As a preliminary to this discussion I would like to indicate, in the context of deeply inelastic scattering off nucleons, a frame which separates current jets from fragmentation jets in a particularly transparent way. To this end take $p \approx (Q/2x, 0, 0, Q/2x)$, $q = (0, 0, 0, -Q)$. Then Sterman-Weinberg current jets are defined by requiring that an amount of energy greater than $(1 - \epsilon)\, Q/2$ go into a cone of half-angle δ opening along the negative z-axis while fragmentation jets are defined by requiring an amount of energy greater than $(1 - \epsilon)\frac{1-x}{x}\frac{Q}{2}$ go into a cone of half-angle δ opening along the positive z-axis as shown in Fig. 10. The cross section for producing current jets or fragmentation jets is completely calculable as a function of δ and ϵ in terms of the total deeply inelastic cross section. In the discussion to follow we shall concentrate on the evolution of current jets as they pass through nuclear matter.

Consider now the evolution of a current jet through nuclear matter in the rest frame of the struck nucleus. The process is illustrated in Fig. 11 where possible final state interactions of the current jet with the nucleus are shown. We know that even in a vacuum the quark struck by the current begins to fragment long before the jet measurement is made. With a jet measurement as described earlier in this section, the mass of the state which the $q + k$ line evolves into is unrestricted up to $Q\delta$. This means $(q + k)^2 \lesssim Q^2\delta^2$. The time scale for the evolution of the $q + k$ line into a state of mass $Q\delta$ is $\tau \approx q{+}k/Q^2\delta^2 \approx 1/mx\delta^2$. For x and δ not too small the evolution of the jet begins in the nuclear matter.

The lowest order perturbative modification of the current jet as it passes through nuclear matter is shown in Fig. 12. p_1 represents a nucleon in the nucleus. Choose an axial gauge where $n = (1, 0, 0, 1)$ and $p \approx (p + m^2/2p, 0, 0, p)$. Then one easily finds

$$\gamma \cdot p\, \gamma_\alpha \gamma \cdot (p - \ell) \left[g_{\alpha\beta} - \frac{\ell_\alpha n_\beta + \ell_\beta n_\alpha}{\ell \cdot n} \right] \approx \gamma \cdot p\, \frac{\ell_-^2}{\ell_-}\, g_{\beta -} \tag{12}$$

where $1/\ell_- = \frac{1}{2}\left(\frac{1}{\ell_- + i\epsilon} + \frac{1}{\ell_- - i\epsilon}\right)$. Now the denominator corresponding to the line $p - \ell$ is $(p - \ell)^2 + i\epsilon - m^2 \approx p^2 - m^2 - \ell_-^2 - 2p_-\ell_+ + i\epsilon$. One sees that there is a trapping of the ℓ_-

contour between the points $\ell_- = p^2 - m^2 - \underline{\ell}^2/2p_+ + i\epsilon$ and $\ell_- = -i\epsilon$. $\underline{\ell}^2$ is limited by normal hadronic masses. If $p^2 = O(m^2)$ the final state scattering is effective. Of course, in the example we are considering $p^2 = m^2$ and $\underline{\ell}^2$ of Eq. (12) is exactly cancelled by the $\underline{\ell}^2$ in the $(p - \ell)^2$ denominator.

However, a further point becomes clear. If $|p^2/m^2| >> 1$ we will obtain a factor $\underline{\ell}^2/p^2 = O(m^2/p^2)$ for interaction of the off-shell quark line with nuclear matter. This is a normal factor which suppresses higher twist effects. We can thus conclude that current jets do suffer final state interactions with the nucleus, but that these interactions can only modify momentum distributions by a few hundred MeV. As soon as a quark or gluon line obtains a mass of a GeV or so it ceases to interact with the nuclear matter.

Thus, for all practical purposes, we may say that a current jet does not significantly interact with a nucleus in which it is produced. This is a rather striking result and tests should be possible in deeply inelastic scattering on heavy nuclei. Of course we should emphasize that our whole discussion presumes that the current quark jets have a momentum in the nuclear rest system larger than $2R\mu^2$ as we described earlier in our discussion of the A-dependence of μ-pair production.

III. Heavy Particle Production at High Energy

The production of heavy particles at high energy, either in hadron-hadron collisions or in deeply inelastic lepton reactions, should be predictable to a reasonable extent by perturbative QCD. In this discussion I shall always suppose the heavy particle is charm, though predictions should be even better for b-particles.

Long ago Georgi-Politzer[17] and Witten[18] argued that charm production in deeply inelastic scattering could be calculated using perturbative QCD. Let me outline crudely how their arguments can be simply understood. Suppose we consider a proton, a bound uud system, moving rapidly. At some instant in time one of the quarks in the proton emits a gluon which then goes into a $c\bar{c}$ system as shown in Fig. 13. We may estimate the lifetime of the $c\bar{c}$ pair by calculating the difference, in old-fashioned perturbation theory, between the incoming energy of the proton, E_p, and the energy of the intermediate state containing the $c\bar{c}$ pair $E_{c\bar{c}}$. One finds $E_p \approx p$ and $E_{c\bar{c}} \approx p + (M_c^2 + \underline{\ell}^2)/2\ell_z + (M_c^2 + (\underline{k} - \underline{\ell})^2)/2(k - \ell)_z$ when $M_c^2 >> m_u^2, m_d^2$. If the charmed quarks carry a finite fraction of the momentum in the proton the lifetime of the $c\bar{c}$ states is $\tau_{c\bar{c}} \approx p/M_c^2$. The lifetime for a normal light quark-antiquark fluctuation in the proton is $\tau_0 \approx p/\mu^2$ where $\mu \approx 350$ MeV. Thus $c\bar{c}$ fluctuations always live a very short time compared to normal light quark and gluon fluctuations. (Interactions which could make the $c\bar{c}$ system survive on a time scale long compared to

p/M_c^2 would require a strength $g^2 M_c^2/\mu^2$.) Now if the $c-\bar{c}$ fluctuation lives only a short time it is clear that the c and $\bar{c}$ never separate. The $c-\bar{c}$ fluctuation is then a short distance and short time effect, exactly the sort of quantity which should be calculable by perturbative QCD.

If a charmed quark is measured in deeply inelastic scattering or if the charmed quark decays into a D by picking up light antiquarks from the vacuum, we may estimate the relevant x-distribution simply by power counting. One finds, from Fig. 14, a charmed quark distribution which goes like $(1-x)^5$ as x goes near 1. This corresponds to central production in an hadronic collision. Such a distribution is a purely perturbative effect and should be reliable to the extent that $\mu^2/M_c^2 << 1$.

There are of course other graphs than that shown in Fig. 14 which contribute to $c-\bar{c}$ production. For example the graph of Fig. 15 is a contribution which is certainly not included in most perturbative QCD calculations. A power counting analysis of that graph yields a behavior $(1-x)^5(\mu^2/M_c^2)^2$. The extra $(\mu^2/M_c^2)^2$ comes about because the extra interactions with the $c-\bar{c}$ system must occur in a time of size p/M_c^2 while their natural time scale is of size p/μ^2.

We conclude that for a single c inclusive reaction, as measured in deeply inelastic scattering or in production of D or $\bar{\Lambda}_c$, perturbation theory should give a reasonable prediction so long as μ^2/M_c^2 terms are not important. We also conclude that c production probabilities should decrease at least as quickly as $(1-x)^5$ as $x \to 1$. In fact leading logarithmic corrections to the Born graphs we have considered here will tend to further suppress the x near 1 behavior.

The x dependence, near $x = 1$, of Λ_c production or of $\bar{D}$ production in proton-proton collisions is easily ascertained. For example for $\bar{D}^0$ production near $x = 1$ we simply need the convolution of the probability for a u-quark in the proton to carry almost all the proton's momentum with the probability for that u-quark to emit a $c-\bar{c}$ pair with the c-quark carrying only a fraction $1 - x$ of the u-quark's momentum. The process is shown in Fig. 16. This immediately leads to a $(1-x)^4$ behavior. For central $\bar{D}$ production, the gluon-gluon fusion model should be accurate. For Λ_c production, illustrated in Fig. 17, near $x = 1$ the relevant probability is given simply by the product of the probability that one of the u-quarks in the proton has a fraction of the proton's momentum of order $1 - x$ times the probability that the other u-quark in the proton emits a $c-\bar{c}$ pair with the $\bar{c}$ having a fraction $1 - x$ of the momentum of the parent quark. One finds a Λ_c production corss section behaving like $(1-x)^2$ as $x \to 1$.

The x near 1 distributions for charmed quarks are much more strongly depressed than appears necessary to fit the ISR data on Λ_c production.[19] Assuming for the moment that this

data is not misleading, what are possible ways out of our analysis? (i) Perhaps non-perturbative effects are important. This would be very surprising since M_c^2 furnishes a mass large enough for us to believe perturbation theory at least to within a factor of two or so. (ii) Perhaps the $(1-x)^n$ behavior we have derived from perturbation theory does not apply until x is extremely close to one. I have examined perturbation graphs and cannot find any effect suggesting that one must be closer to $x = 1$ in order to apply counting rules here than is necessary for processes without charmed particles. In each of these cases the conclusions are necessarily tentative. One really cannot say with certainty that μ^2/M_c^2 effects are necessarily small.

The two most common models dealing with these processes are the intrinsic charm model of Brodsky[20] and collaborators and the flavor excitation model of Barger, Halzen and Keung.[21] In each case these models, which are in many ways similar, are phenomenological. The essential ingredient is a moderately hard charm distribution in the proton. If the Λ_c data is correct then these models may well have the correct physics in their assumptions. Unfortunately, as I have spent the earlier part of this section emphasizing, perturbation theory does not allow a hard enough charm distribution to be consistent with these models. In particular, perturbation theory says the $c\bar{c}$ component does not live long enough to use the Bjorken[22]-Suzuki[23] argument in this circumstance. Thus if the Λ_c data from the ISR are correct, perturbation theory must not be applicable because of large μ^2/M_c^2 effects.

IV. Soft Hadron Production in QCD Jets

When $x \to 0$ single particle inclusive annihilation cross sections in e^+e^- collisions are no longer governed by a straightforward application of the renormalization group. This shows up, for example, in a series of the form

$$\gamma_n(g^2) = \frac{g^2}{n-1} \sum_{r=1}^{\infty} c_r \left(\frac{g^2}{(n-1)^2}\right)^{r-1} + \text{less singular terms} \qquad (13)$$

for the anomalous dimension matrix. Several people[24-27] have suggested that a complete solution to the axial gauge ladder graphs might be a way to go beyond the renormalization group and obtain small-x results. Such an approach has been successful in obtaining Sudakov effects as $x \to 1$. Following this suggestion one obtains an average multiplicity of produced hadrons growing like an exponential of $\sqrt{\ln Q^2}$. Such an increase comes from a square root branch point of $\gamma_n(g^2)$ in n after summing the leading terms in the series indicated in (13).

However, in contrast to the $x \to 1$ case, it now appears that the above procedure gives the correct form of γ_n, but not the correct values of the parameters appearing in the square root. The origin of this difficulty is that non-planar graphs are just as important as planar

graphs. We may understand this in the following way. The average multiplicity is determined by

$$\bar{n}(Q^2)\,\sigma = \int 2E \frac{d\sigma}{d^3p} \frac{d^3p}{2E} \tag{14}$$

or

$$\frac{4\bar{n}(Q^2)}{\pi Q^2} = \int_{2P/Q}^{1} 2E \frac{d\sigma}{d^3p}\, x dx \tag{15}$$

where $d\sigma/d^3p$ is the inclusive cross section for producing a particle of momentum p and mass P. p corresponds to a fraction, x, of the maximum possible momentum of the produced particle. In (15) factors of $1/x^2 \ln^r 1/x$ in $2E(d\sigma/d^3p)$ get changed into $\ln^{n+1} Q/P$ factors in $\bar{n}$. Thus terms which are non-leading in $2E(d\sigma/d^3p)$ as far as powers of $\ln Q^2$ are concerned may have additional powers of $\ln 1/x$ and be part of the leading series in $\ln Q^2$ as far as $\bar{n}(Q^2)$ is concerned. This is exactly what happens for non-planar graphs.

An explicit computation[28] through order g^6 gave a singlet anomalous dimension consistent with

$$\gamma_n = \frac{1}{4}\left[-(n-1) + \sqrt{(n-1)^2 + \frac{8\alpha c_A}{\pi}}\right] . \tag{16}$$

(Planar graphs give a similar result except that the 4 and 8 in (16) are replaced by 2 and 4 respectively.) Recently,[29] it has been shown that Eq. (16) correctly gives all the terms in the leading series of powers of $g^2/(n-1)^2$ in QCD. It is an important task to show that non-leading terms preserve the square root form of the anomalous dimension so that one may have real confidence that Eq. (16) represents the actual values of the anomalous dimension when g^2 and $n-1$ are small. Before briefly describing how the result of Ref. 29 was obtained, let me first give the physics results which follow from (16).

We may now use factorization, which states

$$(Q^2)^2 \int 2E \frac{d\sigma}{d^3p} x^n dx \xrightarrow[Q^2\to\infty]{} A_n E_n(Q^2) , \tag{17}$$

and the renormalization group, which gives

$$E_n(Q^2) = e^{\int_{\mu^2}^{Q^2} \frac{d\lambda^2}{\lambda^2} \gamma_n[g^2(\lambda^2)]} \tag{18}$$

to find

$$\bar{n}(Q^2) \propto e^{\int_{\mu^2}^{Q^2} \frac{d\lambda^2}{\lambda^2} \gamma_1[g^2(\lambda^2)]} . \tag{19}$$

Although $\gamma_1(g^2)$ does not make sense order by order in perturbation theory, the form (16) does make sense evaluated at $n = 1$, so one gets $\gamma_1(g^2) = \sqrt{\alpha c_A/2\pi}$. One easily finds

$$\bar{n}(Q^2) \propto e^{\sqrt{\frac{2c_A}{\pi b} \ln Q^2}} \tag{20}$$

with $b = \frac{33 - 2n_f}{12\pi}$. One may also use (16) to solve for $d\sigma/dx$ at small x. The result which emerges is

$$x\frac{d\sigma}{dx} \propto \frac{e^{\sqrt{\frac{2c_A}{\pi b} \ln Q^2}}}{\sqrt{\ln^{3/2} Q^2}} \; e^{-3\sqrt{\frac{8c_A}{\pi b}} \frac{(\frac{1}{4}\ln Q^2 - \ln\frac{1}{x})^2}{\ln^{3/2} Q^2}} \tag{21}$$

so long as $(\frac{1}{4}\ln Q^2 - \ln\frac{1}{x})^2/\ln^2 Q^2 \ll 1$. Perhaps at LEP the decrease in $x(d\sigma/dx)$ when $\ln\frac{1}{x} > \frac{1}{2}\ln Q^2$ will be seen. This would be most striking.

Let me now outline how Eq. (16) is obtained. One works with $x(d\sigma/dx)$. The leading singularities in γ_n come completely from gluonic interactions. As a device to get these singularities, without having to discuss fermions at all, it is convenient to introduce a gauge invariant current $j(x) = F_{\mu\nu}(x) F_{\mu\nu}(x)$ which is used to produce the jets in which the particle of momentum fraction x is measured. One writes

$$x\frac{d\sigma}{dx} = \sum_{r=1}^{\infty} (g^2)^r \sum_{\ell=0}^{2r-1} c_\ell (\ln Q^2/P^2)^{2r-\ell-1} (\ln\frac{1}{x})^\ell \tag{22}$$

for the most singular terms as $x \to 0$ and $Q^2 \to \infty$. (Recall that $\ln\frac{1}{x} \propto \ln Q^2$ in the region of dominant particle production.) Suppose, at a given order in perturbation theary, that $N+1$ particles (gluons) of momenta $p, k_1, k_2, \cdots k_N$ are produced. The results which lead to (16) are first that p is the smallest momentum in the overall center of mass system, and second if

$$p \ll k_1 \ll k_2 \ll \cdots \ll k_{N-1} \ll k_N = Q/2 \tag{23a}$$

then

$$\theta(\vec{p}, \vec{k}_1) \ll \theta(\vec{k}_1, \vec{k}_2) \ll \cdots \ll \theta(\vec{k}_{N-2}, \vec{k}_{N-1}) \ll \theta(\vec{k}_{N-1}, \vec{k}_N) \tag{23b}$$

as far as the region of phase necessary for calculating the leading singularities is concerned. The above angular ordering was suggested independently in Ref. 28 and Ref. 30, and was proved for all leading terms in Ref. 29. Once (23) is known it follows immediately that the leading terms in $x(d\sigma/dx)$ are obtained by taking the ladder graphs of Fig. 18 and evaluating them with the constraints (23). It should be emphasized that the above constraints do not follow from kinematic considerations alone, but are dynamical restrictions outside the ladder graphs themselves.

The general proof of (23) given in Ref. 29 is quite intricate. However the idea is

relatively simple. Let me state the idea of the proof in a few words.

In order to get the maximum singularity at a given order in perturbation theory all momenta, both real and virtual, must be strongly ordered. (In the leading singularity approximation virtual lines are not very far from mass shell. Strong ordering for these lines can be done either in energy or in momentum since there is no difference in the resulting orderings.) A gluon of momentum k_i can be emitted from a line harder than itself and can emit lines with softer momentum. (In a region of strongly ordered momenta we need only consider trilinear gluon couplings.) Suppose a line k_i is emitted from a line k_j, $k_i \ll k_j$ of course. The vertex for this emission is shown in Fig. 19. If we include $1/\sqrt{2E}$ factors for the emitting line, the dominant term in the vertex is given by $(2k_{j\alpha}/2k_{jo})\, g_{\beta\gamma}\, igT^a_{bc}$ in axial gauge. This vertex factor is the number density current of the line k_j multiplied by a color rotation factor $(c \mid Q^a \mid b)$. If a soft line k_i makes an angle θ_{iI} with a set of hard lines $k_j \in I$ which is larger than the angles, $\theta_{jj'}$, between the lines in I then it is clear that the line k_i measures, and color rotates, the total color current of the lines in I when k_i interacts with those lines.

Recall that the total cross section $\sigma(Q^2)$ has only logarithms coming from $\alpha(Q^2)$. The higher logarithms in $x(d\sigma/dx)$, soft and collinear logarithms, are caused by the detection of the line p. Thus if the p line can be viewed as measuring the color charge of those hard lines with which it makes a large angle, the emission of the p line will be ineffectual in producing collinear singularities. (This is exactly the way a Sterman-Weinberg jet cross section works. In such a jet a conserved quantity, energy, is the limiting factor determining what is a jet event. Such a measurement is insensitive to collinear emission of gluons and so only logarithms from the running coupling appear. A similar situation occurs here. If the total color current of a set of gluons, I, is being measured by a line p, then all collinear logarithms in I will be lost.) To get the maximum number of collinear and soft emission logarithms it is necessary that the softest gluons make the smallest angles with each other. This is exactly what Eq. (23) states.

V. Soft Gluons and Factorization in μ-Pair Production

One of the most widely discussed topics in QCD in the past year or so has been the question of factorization in μ-pair production. A few years ago calculations done in quark-antiquark $\to \mu^+ + \mu^- + X$ showed[31,32] that at high energy factorization worked through the two-loop level at least as far as logarithmic terms are concerned. Recently, however, Bodwin, Brodsky and Lepage (BBL)[16] suggested that such a factorization would break down in quark-hadron scattering at the two-loop level in soft gluon corrections. It was later suggested that Sudakov corrections might suppress this non-factorization.[33]

In these lectures I am taking the position that the BBL discussion is correct in perturbation theory. I shall then show why I feel Sudakov corrections should ultimately suppress this non-factorization, though at what values of Q^2 is not completely clear. The reader should be warned, however, that many QCD theorists are not ready to accept either of the above statements on the basis of the arguments that have so far been given. Before discussing the μ-pair situation, let me go back a few steps and talk about other processes where soft gluon effects might come in, but where in fact they cancel order by order in perturbation theory.

A. Soft Gluon Cancellations in e^+-e^- Collisions[34]

Consider a two-jet process in an e^+-e^- collision as illustrated in Fig. 20. In that figure the particles of the jet are the two blobs, while soft gluons are shown connecting the two jets. We imagine working in an axial gauge with $n^2 \neq 0$ and grouping the quarks and gluons into four categories. (i) Quarks and gluons collinear with the positive z-axis, jet (i); (ii) A similar grouping for the opposite going jet; (iii) Hard gluons, which have been reduced to a point; (iv) Soft gluons, shown connecting jet (i) and jet (ii). Let $\hat{p}_1$ be a light-like vector along the (i) jet direction. Then $\hat{p}_1^2 = 0$, $\hat{p}_{1+} \neq 0$. Let $\hat{p}_2$ be a similar vector for the (ii) jet. A soft gluon hooking into jet (i) measures the charge of that jet and picks up a factor $\hat{p}_{1\alpha}$. Other than the charge and direction of the jet, the soft gluon is insensitive to the jet properties. Now in a jet process one does not need to require that physical hadrons be formed in order to measure the jet energy distribution. This means that a jet formation is a short time process. In the center-of-mass system it takes a time of order c/Q to properly define the jet. (This constant c depends in detail on our demand of angular resolution. This is the same ambiguity in what we have called a collinear gluon in (i) and (ii) above. In this heuristic discussion I shall not make the discussion more precise and so c must be left somewhat ill-defined.) But, such a short time process cannot involve soft gluons at all. Thus the different cuts through the soft gluons shown in Fig. 20 must cancel.

Let us now consider the slightly more complicated process of $e^+ + e^- \rightarrow$ hadron (p_1) + hadron (p_2) + x as shown in Fig. 21. Now we show the p_1 line with its accompanying jet of collinear particles, the p_2 line with its accompanying jet of collinear particles and the soft gluon connections. We suppose that p_1 and p_2 are almost back to back, but are integrated over small angular regions about the $\pm$ z-axis. This is a two-jet event where specific particles, neutral in color, are measured in jet (i) and jet (ii). The soft gluon connections to the jets are exactly the same as in our previous discussion where the hadrons, p_1 and p_2, were absent. (Recall that these connections depend only on the direction and color of the jets.) Thus soft gluons must also cancel in this process.[34] Now, however, the cancellation is very non-trivial in that a long time process is involved in order to define the hadrons as on-mass-shell particles. The above is a

rough description of the cancellation first discussed by Collins and Sterman.

B. Soft Gluon Interactions with Jets in Nuclear Matter

Earlier in Sec. II we have discussed the evolution of a current jet in nuclear matter. We concluded there that soft gluon interactions between the jet and the nuclear matter were small. In this section I would like to argue this result in a slightly different and in a more technical way. To that end consider the graph shown in Fig. 22 contributing to the time-ordered deeply inelastic amplitude. We suppose the target is a nucleus, A , and that $P = (Am, 0, 0, 0) = Ap$. We also take $q_\mu = (q-mx, 0, 0, q)$ so that q_+ is large and $q_- = -xp_-$ with x the conventional Bjorken variable. Finally we choose a light cone axial gauge with $\eta_+ = 1$, $\eta_- = \underline{\eta} = 0$. Consider the denominators associated with the line through which the q momentum runs. We may write

$$\frac{1}{\left[(q+k)^2+i\epsilon\right]\left[(q+k+\ell_1)^2+i\epsilon\right]\left[(q+k+\ell_1+\ell_2)^2+i\epsilon\right]} \approx$$

$$\frac{1}{\left[2q_+(-xp_-+k_-)-\underline{k}^2+i\epsilon\right]\left[2q_+(-xp_-+k_-+\ell_{1-})-(\underline{k}+\underline{\ell}_1)^2+i\epsilon\right]\left[2q_+(-xp_-+k_-+\ell_{1-}+\ell_{2-})-(\underline{k}+\underline{\ell}_1+\underline{\ell}_2)^2+i\epsilon\right]}.$$

We may normally choose k_- so that $-xp_- + k_-$, $-xp_- + k_- + \ell_{1-}$ and $-xp_- + k_- + \ell_{1-} + \ell_{2-}$ are not particularly small. Thus the addition of the two gluons gives an additional $\frac{1}{q_+^2} \propto \frac{1}{(Q^2)^2}$ factor. The only way to conpensate this factor is to get q_+ numerator factors. But, the axial gauge propagator is proportional to

$$g_{\alpha\beta} - \frac{\eta_\alpha \ell_{1\beta} + \eta_\beta \ell_{1\alpha}}{\eta \cdot \ell}$$

which vanishes when $\alpha = -$. Thus we have reached a standard conclusion that there are no gluonic corrections to one of the fermionic lines connecting the two currents in deeply inelastic scattering at the dominant twist level.

Our argument for the smallness of the amplitude has so far been only for the time-ordered product. However, the structure functions are given by the imaginary part of the time-ordered product so the lack of gluonic corrections, in fact, holds also for the structure functions arising from three separate terms, shown in Fig. 23. The first observation to note is that the separate discontinuities of Fig. 23 are not small. The point being that a denominator like

$$\frac{1}{2q_+(-xp_- + k_- + \ell_{1-}) - (\underline{k}+\underline{\ell})^2 + i\epsilon} = \frac{1}{2q_+\ell_{1-} - (\underline{k}+\underline{\ell})^2 + \underline{k}^2 + i\epsilon}$$

coming from the cut across the $(q+k)^2$ line can be trapped by the $1/\ell_{1-} - i\epsilon$ coming from the

axial gauge denominator. If the ℓ_{1-} contour is used to pick up the $\ell_{1-} = 0$ pole, say, then the $1/(q+k+\ell_1)^2$ denominator becomes $1/\underline{k}^2 - (\underline{k}+\underline{\ell})^2 + i\epsilon$ which is not large in general. We conclude that the soft gluonic corrections cancel in the various intermediate states contributing to the structure function, but that they may make a contribution to a definite cut in a particular graph.

If, for example, we require that the current jet consist of only a single quark with zero transverse momentum it is easy to see that the different cuts contributing to that cross section do not cancel. The problem here is that a zero transverse momentum requires $\underline{k}$ small in all the cuts and the translations of transverse momentum, by $\underline{\ell}_1$ and $\underline{\ell}_2$, necessary to get the zero measured transverse momentum to not give the same relative contributions as the integrated distributions which occur in the total cross section. However, if we allow the measured fermion in the current jet to have a transverse momentum $|\underline{k}_i| < Q_0$, then the cancellation among the various cuts is effective up to a correction of size μ^2/Q_0^2 with μ the typical size of $|\underline{\ell}_i|$. In a jet measurement one fixes an angular cone in which particles are measured. In our example this is the same as a restriction on $|\underline{k}_i|$. In fact a normal Sterman-Weinberg jet corresponds to restricting the transverse momentum of the measured quark, in our example, to be less than a fraction of Q. Thus we see that for a jet measurement soft gluonic corrections do not give any but higher twist contributions. This confirms our previous conclusion that current jets pass through nuclear matter without interaction with that matter.

C. Soft Gluon Corrections in the Drell-Yan Process

Following Bodwin, Brodsky and Lepage (BBL)[16] we shall consider quark-hadron scattering as shown in Fig. 24. For simplicity we consider the solid lines to be scalar particles and the dotted line a point scalar. We begin by considering a soft gluon correction, the line ℓ in Fig. 24. We suppose $p_1 = (p_1 + \frac{m^2}{2p_1}, 0, 0, p_1)$ and we use a light cone gauge with $\eta = \sqrt{2}(1, 0, 0, 1)$. Then our discussion in part B of this section has shown that there is a non-trivial contribution from this soft gluon exchange, due to the trapping of the contours in the ℓ_- plane coming from the factors $1/2p_{1+}\ell_- - \underline{\ell}^2 + i\epsilon$ and $1/\ell_- - i\epsilon$ corresponding to the denominator of the $p_1 + \ell$ - line and the axial gauge denominator respectively. Let us go through this explicitly. We first note that in the axial gauge projection, $d_{\alpha\beta} = g_{\alpha\beta} - (\eta_\alpha \ell_\beta + \eta_\beta \ell_\alpha)/\ell \cdot \eta$ the $\alpha = -$ term is absent. Since the β index must be $+$ in order not to have a small result for the graph of Fig. 24, we may write $d_{\alpha\beta} \to -\left.\frac{\eta_\alpha \ell_\beta + \eta_\beta \ell_\alpha}{\ell_-}\right|_{\alpha \neq -}$. Now we shall see in a moment that the $p - k + \ell$ line will be put on-shell by contour distortion so the ℓ_β term may be dropped. Thus $d_{\alpha\beta} \to -\left.\frac{\eta_\beta \ell_\alpha}{\ell_-}\right|_{\alpha \neq -}$. The ℓ_- denominator is taken to be a principal value. Only $\frac{1}{2}(1/\ell_- - i\epsilon)$ is effective, so we may write $d_{\alpha\beta} \to -\frac{1}{2}\left.\frac{\eta_\beta \ell_\alpha}{\ell_- - i\epsilon}\right|_{\alpha \neq -}$.

Now we distort the ℓ_- contour in the lower half plane so as to pick up the singularity at $\ell_- = \underline{\ell}^2/2p_{1+}$. Now that the $(p_1 + \ell)$ line has been put on-shell we can write $d_{\alpha\beta} \to -\frac{1}{2}\frac{\eta_\beta \ell_\alpha}{\ell_-} + \frac{1}{2}\eta_\beta \tilde{\eta}_\alpha$ with $\tilde{\eta} = \frac{1}{\sqrt{2}}(1, 0, 0, -1)$ and the ℓ_α term can be dropped to give $d_{\alpha\beta} \to \frac{1}{2}\eta_\beta \tilde{\eta}_\alpha = \tilde{d}_{\alpha\beta}$ with the understanding that only the pole term $(p_1 + \ell)^2 = 0$ is to be taken. Now the ℓ_+ contour can be done by distorting the contour into the lower half plane to pick up the singularity at $\ell_+ = (\underline{k}-\underline{\ell})^2/2(p-k)_- - (p-k)_+$. Finally, let us write the full answer for the graph in Fig. 24 bearing in mind that all particles except the gluons are scalars. We have found

$$G = \frac{i\lambda_g^2 2}{(2\pi)^8}\int \frac{d^4k d^4\ell\,(2p_1+\ell)_\alpha (2p-2k+\ell)_\beta d_{\alpha\beta}(\ell)\, 2\pi\delta((p-k)^2)\, f((p_1+k)^2)}{[\ell^2+i\epsilon][(p_1+\ell)^2+i\epsilon][(p-k+\ell)^2+i\epsilon][(k-\ell)^2+i\epsilon](k^2+i\epsilon)}$$

$$= \frac{-i\lambda_g^2 2}{(2\pi)^6}\int \frac{d^4k d^2\underline{\ell}}{\underline{\ell}^2}\,\frac{2p_{1\alpha}2(p-k)_\beta \tilde{d}_{\alpha\beta}}{4p_1\cdot(p-k)}\,\frac{2\pi\delta((p-k)^2)\, f((p_1+k)^2)}{(k-\ell)^2 k^2}\,. \qquad (24)$$

Thus

$$G = \frac{-i\lambda_g^2 2}{(2\pi)^5}\int \frac{d^4k d^2\underline{\ell}}{2\underline{\ell}^2}\,\frac{2\pi\delta((p-k)^2)\, f((p_1+k)^2)}{k^2(k-\ell)^2} \qquad (25)$$

where f represents the vacuum polarization involving the μ-pair and k^2 and $(k-p)^2$ are to be evaluated using the mass shell conditions determining $\ell_\pm$. We need go no further in evaluating G because it is clear G is purely imaginary in which case it is exactly cancelled by a graph identical to that in Fig. 24 except that the gluon correction comes to the right of the cut. Thus, for one soft gluon there is a cancellation of soft effects in the cross section.

Now consider the graph shown in Fig. 25. Exactly as before we may replace $d_{\alpha_1\beta_1}(\ell_1)$ by $\frac{1}{2}\tilde{\eta}_{\alpha_1}\tilde{\eta}_{\beta_1} = \tilde{d}_{\alpha_1\beta_1}$ with the understanding that the ℓ_{1-} contour encloses the pole at $\ell_{1-} = -\underline{\ell}_1^2/2p_{1+}$ and replace $d_{\alpha_2\beta_2}(\ell_2)$ by $\tilde{d}_{\alpha_2\beta_2}$ where the contour in the ℓ_{2-} encloses the pole at $\ell_{2-} = \underline{\ell}_1^2/2p_{1+} - (\underline{\ell}_1+\underline{\ell}_2)^2/2p_{1+}$. Now, however, the argument for these replacements is more subtle. We begin by realizing that $d_{\alpha_2\beta_2}(\ell_2) \to -\left.\frac{\eta_{\alpha_2}\ell_{\beta_2} + \eta_{\beta_2}\ell_{\alpha_2}}{\ell_{2-}}\right|_{\alpha_2 \neq -}$.

Further only the $\ell_{2-} - i\epsilon$ part of the principal value is effective so

$d_{\alpha_2\beta_2} \to -\frac{1}{2}\left.\frac{\eta_{\alpha_2}\ell_{\beta_2} + \eta_{\beta_2}\ell_{\alpha_2}}{\ell_{2-} - i\epsilon}\right|_{\alpha_2 \neq -}$. Now we distort the ℓ_{2-} contour to pick up the pole at $\ell_{2-} = -\ell_{1-} - (\underline{\ell}_1+\underline{\ell}_2)^2/2p_{1+}$. Next we distort the ℓ_{1+} contour to pick up the pole

in $(p-k+\ell_1+\ell_2)^2$. At this point we have isolated an on-shell scattering as shown in Fig. 26. Now this on-shell scattering has a real and an imaginary part. The real part must cancel between the present graph, Fig. 25, and the graph where the two lines appear to the right of the cut, much as for the single gluon exchange. The imaginary part of the graph in Fig. 26 is determined by the rule $\mathrm{Im} = -i/2\ \mathrm{disc}$ where one now uses Cutkosky rules to evaluate disc. The effect of taking the imaginary part is equal to a factor of $1/2$ times the result of distorting the ℓ_{1-} contour so as to pick up only the pole at $\ell_{1-} = -\underline{\ell}_1^{\,2}/2p_{1+}$ and distorting the ℓ_{2+} contour so as to pick up only the pole $\ell_{2+} = -(p-k)_+ - (\underline{k}-\underline{\ell}_2)^2/2(p-k)_-$. After all this has been done we find that we have set

$$\int \frac{d\ell_{1+}d\ell_{1-}d\ell_{2+}d\ell_{2-}(2p_1+\ell_1)_{\alpha_1}(2p_1+2\ell_1+\ell_2)_{\alpha_2}(2p-2k+2\ell_1+\ell_2)_{\beta_1}(2p-2k+\ell_2)_{\beta_2}d_{\alpha_1\beta_1}(\ell_1)d_{\alpha_2\beta_2}(\ell_2)}{\ell_1^2\ell_2^2[(p+\ell_1)^2+i\epsilon][(p_1+\ell_1+\ell_2)^2+i\epsilon][(p-k+\ell_2)^2+i\epsilon][(p-k+\ell_1+\ell_2)^2+i\epsilon]}$$

$$= \frac{1}{2}\ \frac{(2\pi)^4}{4\underline{\ell}_1^{\,2}\underline{\ell}_2^{\,2}}\ . \qquad (26)$$

Now we consider also the graph shown in Fig. 27. The evaluation of this graph proceeds as for the graph of Fig. 24. We find that effectively we have made the same replacement as in Eq. (26) except for an additional factor of 2 and a $-$ sign. Now we add the contribution of the graph in Fig. 25. Begin by supposing that we are dealing with abelian gluons. Then there would be a cancellation if the lines involving k were equal. That is we need

$$\frac{1}{k^2(k-\ell_1-\ell_2)^2} = \frac{1}{(k-\ell_1)^2}\ \frac{1}{(k+\ell_2)^2}\ .$$

If we allow the translation $\underline{k} \to \underline{k}+\underline{\ell}_2$ on the left hand side, this is a correct equation as can be verified by using the appropriate δ-functions for the graphs in question. That is, for the graph in Fig. 25 one uses

$$k^2 = 2p_+k_- - \underline{k}^2\ \frac{p_-}{(p-k)_-}\ ,$$

$$(k-\ell_1-\ell_2)^2 = 2p_+k_- - (\underline{k}-\underline{\ell}_1-\underline{\ell}_2)^2\ \frac{p_-}{(p-k)_-}$$

and

$$(k-\ell_1)^2 = 2p_+k_- - (\underline{k}-\underline{\ell}_1)^2\ \frac{p_-}{(p-k)_-}\ ,$$

$$(k+\ell_2)^2 = 2p_+k_- - (\underline{k}+\underline{\ell}_2)^2\ \frac{p_-}{(p-k)_-}$$

for the graph in Fig. 27. Thus for an abelian theory we have verified that the graphs in Fig. 25 and Fig. 27 cancel.

In the non-abelian case the calculation is identical except for color factors. The color factors are most easily seen by considering the "hard part" of the graph as shown in Fig. 28. We may write the color indices in terms of a singlet exchange, $\delta_{ab}\delta_{cd}$, and an octet exchange, $(\lambda_i/2)_{ba}(\lambda_i/2)_{dc}$, where we have gone back to a case with fermions in the fundamental representation for the color factors. The singlet exchange behaves exactly as in the abelian model as the color factors are the same for the graph of Fig. 25 as they are for the graph of Fig. 27. However, the octet case is different and the two graphs do not cancel. This is the non-factorization of (BBL). It is physically clear, however, that one cannot have a high energy reaction which involves a color exchange, the octet exchange we have just been discussing, which is not suppressed due to an incomplete cancellation between real and virtual hard collinear gluons. Thus we expect this non-factorizing part of the Drell-Yan process to be suppressed by a Sudakov factor. Whether this suppression is effective at present energies is at this moment a phenomenological question.[16]

Acknowledgements

I have benefited from many discussions with my colleagues on the topics included here. In particular I have had a number of stimulating conversations with Stanley Brodsky and Peter Lepage on the subject of the interactions of hadrons and currents with nuclei.

References

(1) For a review see A. H. Mueller, Physics Reports 73 (1981) 237 and G. Altarelli, Physics Reports 81 (1982) 1.

(2) G. Farrar and D. Jackson, Phys. Rev. Letters 43 (1979) 246.

(3) V. L. Chernyak and A. R. Zhitniskii, Pisma Zh. Exsp. Theo. Fiz. 25 (1977) 544.

(4) A. Efremov and A. Radyushkin, Phys. Letters 94B (1980) 245.

(5) S. J. Brodsky and G. P. Lepage, Phys. Rev. Letters 43 (1979) 545; Phys. Letters 87B (1979) 359.

(6) A. Duncan and A. H. Mueller, Phys. Rev. D21 (1980) 1636; Phys. Letters 90B (1980) 159.

(7) For a more complete set of references see Ref. 1.

(8) S. J. Brodsky and G. Farrar, Phys. Rev. Letters 31 (1973) 1153.

(9) P. Landshoff, Phys. Rev. D10 (1974) 1024.

(10) M. Goodman et al., Phys. Rev. Letters 47 (1981) 293.

(11) V. N. Gribov, JETP 30 (1970) 709.

(12) S. J. Brodsky and J. Pumplin, Phys. Rev. 182 (1969) 1794.

(13) J. Bell (unpublished).

(14) G. Grammar and J. D. Sullivan in Electromagnetic Interactions of Hadrons, Vol.2, ed. A. Donnachie and G. Shaw, Plenum (1978).

(15) J. D. Bjorken (Private Communication).

(16) A-dependence of μ-pair production has been discussed by G. Bodwin, S. J. Brodsky and G. P. Lepage, Phys.Rev.Letters 47 (1981) 1799. An extended version of their work is in preparation by the above authors.

(17) H. Georgi and H. D. Politzer, Phys.Rev. D14 (1976) 1829.

(18) E. Witten, Nucl.Phys. B104 (1976) 345.

(19) The experimental situation on heavy quark production in hadronic collisions is impossibly complex. There are a number of excellent reviews however. In particular the review by L. Montanet at this conference should be helpful.

(20) S. J. Brodsky, P. Hoyer, C. Peterson and N. Sakai, Phys.Letters 93B (1980) 451.

(21) V. Barger, F. Halzen and W. Y. Keung, Phys.Rev. D24 (1981) 1328; ibid., D25 (1982) 112.

(22) J. D. Bjorken, Phys.Rev. D17 (1978) 171.

(23) M. Suzuki, Phys.Letters 71B (1977) 139.

(24) A. Bassetto, M.Ciafaloni and G. Marchesini, Nucl.Phys. B163 (1980) 477.

(25) D. Amati, A. Bassetto, M. Ciafaloni, G. Marchesini, G. Veneziano, Nucl.Phys. B173 (1980) 429.

(26) K. Konishi, Rutherford Report RL 79-035 (1979).

(27) W. Furmanski, R. Petronzio and S. Pokorski, Nucl.Phys. B155 (1979) 253.

(28) A. H. Mueller, Phys.Letters 104B (1981) 161.

(29) A. Bassetto, M. Ciafaloni, G. Marchesini and A. H. Mueller, University of Florence Preprint 82/11.

(30) B. I. Ermolaev and V. S. Fadin, JETP Letters 33 (1981) 269.

(31) R. Doria, J. Frenkel and J. C. Taylor, Nucl.Phys. B168 (1980) 93.

(32) C. di Lieta, S. Gendron, I. Halliday and C. Sachrajda, Nucl.Phys. B183 (1981) 223.

(33) A. H. Mueller, Phys.Letters 108B (1982) 355.

(34) J. Collins and G. Sterman, Nucl.Phys. B185 (1981) 172.

Figure Captions

Fig. 1. Quark evolution in the pion form factor.

Fig. 2. Elastic scattering in the Brodsky-Farrar picture.

Fig. 3. The Landshoff graph.

Fig. 4. The hadronic fluctuation of a photon interacting with a nucleus.

Fig. 5. The nuclear structure function in the ∞-momentum frame of the nucleus.

Fig. 6. The longitudinal size of the valence quarks in a nucleus.

Fig. 7. Different paths of evolution of quarks in the nuclear structure function.

Fig. 8. Path (2) as viewed in the rest frame of the nucleus.

Fig. 9. μ-pair production on a nucleus, A.

Fig. 10. Separation of current and fragmentation jets.

Fig. 11. The possible interactions of a current jet as it goes through a large nucleus.

Fig. 12. A single interaction of an outgoing quark with a nucleus.

Fig. 13. A c-$\bar{c}$ fluctuation in a proton.

Fig. 14. The c-distribution in the proton.

Fig. 15. A higher twist contribution to the c-distribution in the proton.

Fig. 16. $\bar{D}$ production near $x = 1$.

Fig. 17. Λ_c production near $x = 1$.

Fig. 18. Gluon ladders induced by a current $(F_{\mu\nu})^2$.

Fig. 19. A QCD vertex.

Fig. 20. Soft gluon interactions between two jets.

Fig. 21. Soft gluon interactions in $\ell^+ + \ell^- \to k(p_1) + k(p_2) + \Sigma$.

Fig. 22. A two gluon exchange in deeply inelastic scattering.

Fig. 23. Different cuts of Fig. 22.

Fig. 24. An active-spectator interaction in μ-pair production.

Fig. 25. A two gluon active-spectator interaction.

Fig. 26. An elastic quark-quark scattering.

Fig. 27. A two soft gluon correction to μ-pair production.

Fig. 28. The "hard part" of the μ-pair production.

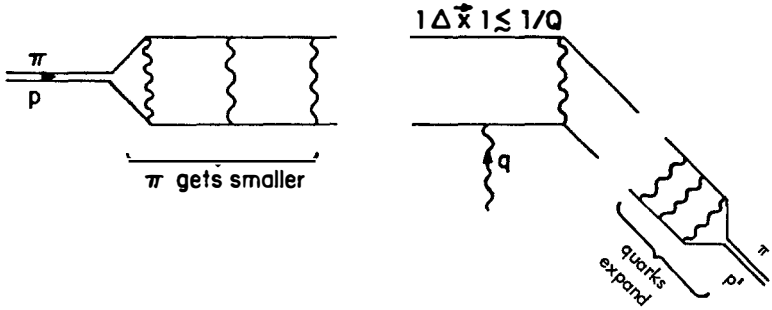

Fig. 1

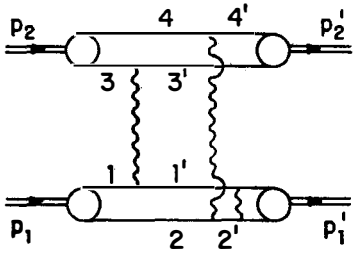

Fig. 2

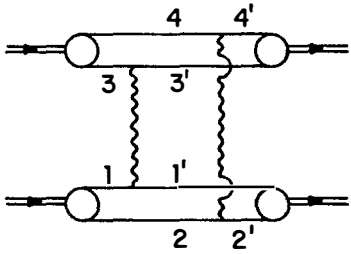

Fig. 3

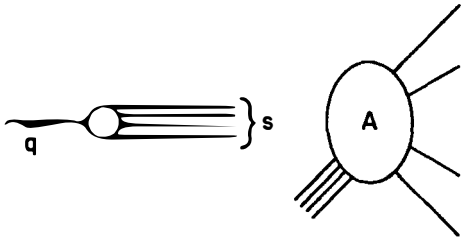

Fig. 4

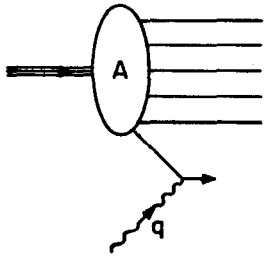

Fig. 5

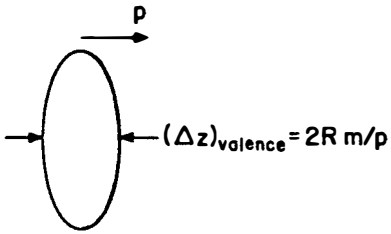

Fig. 6

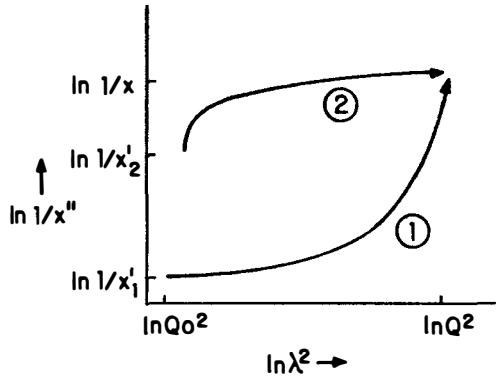

Fig. 7

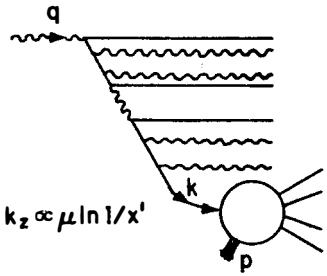

Fig. 8

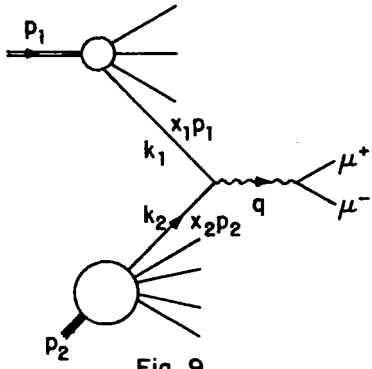

Fig. 9

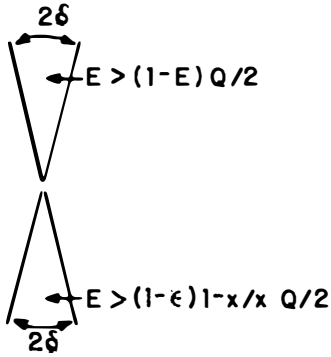

Fig. 10

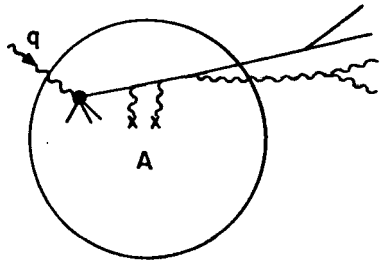

Fig. 11

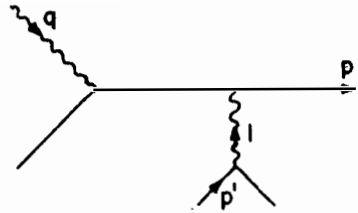

Fig. 12

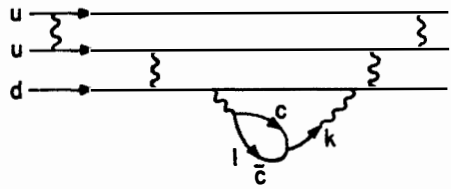

Fig. 13

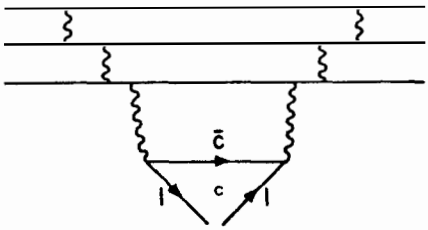

Fig. 14

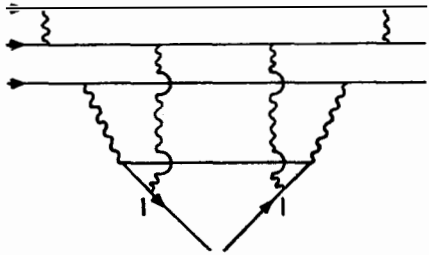

Fig. 15

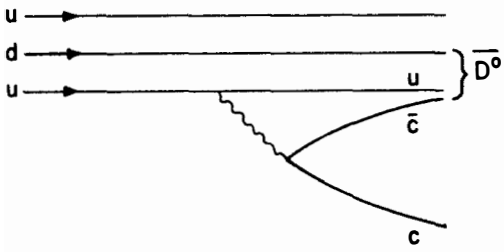

Fig. 16

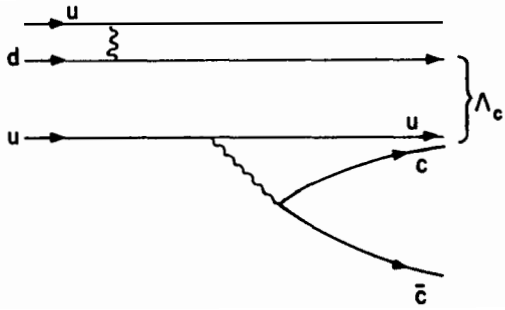

Fig. 17

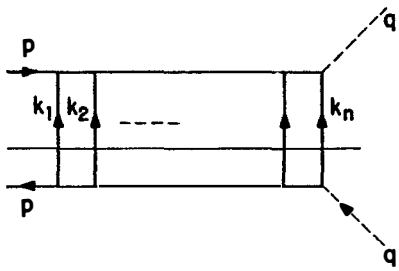

Fig. 18

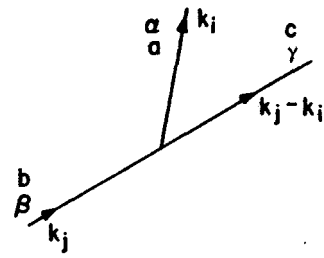

Fig. 19

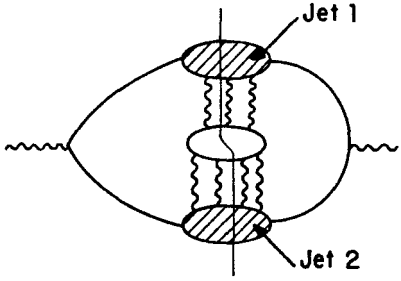

Fig. 20

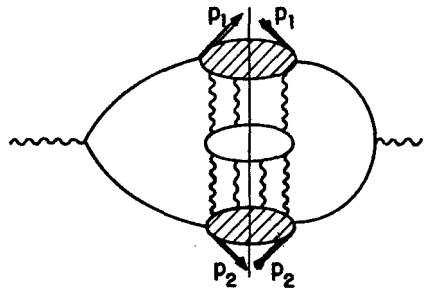

Fig. 21

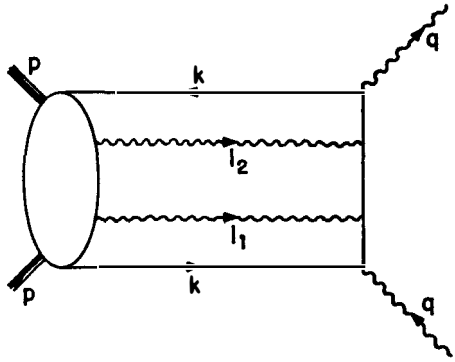

Fig. 22

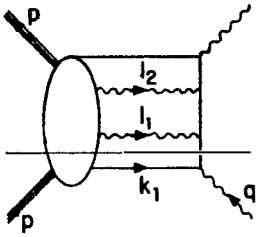

Fig. 23a

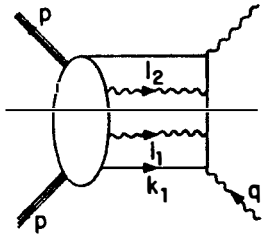

Fig. 23b

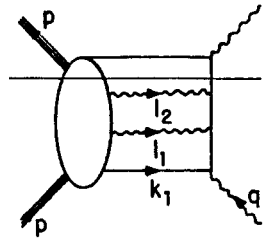

Fig. 23c

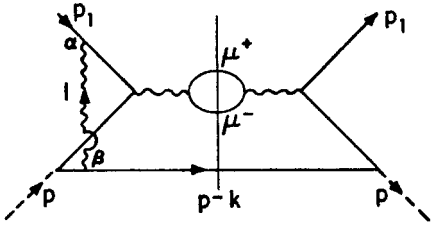

Fig. 24

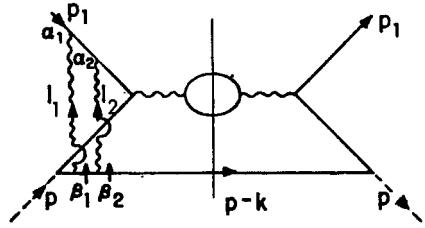

Fig. 25

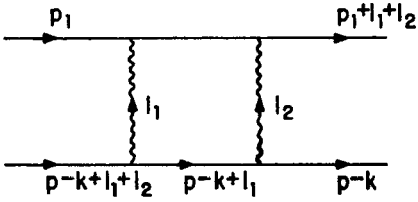

Fig. 26

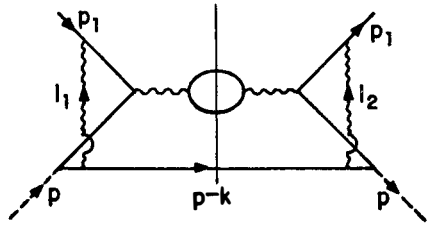

Fig. 27

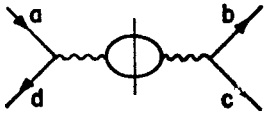

Fig. 28